Sensor Placement for On-Orbit Modal Identification and Correlation of Large Space Structures

Daniel C. Kammer*
University of Wisconsin, Madison, Wisconsin 53706

A method is presented for the selection of a set of sensor locations from a larger candidate set for the purpose of on-orbit identification and correlation of large space structures. The method ranks the candidate sensor locations according to their contribution to the linear independence of the target modal partitions. In an iterative manner, locations that do not contribute significantly are removed. The final sensor configuration tends to maximize the trace and determinant and minimize the condition number of the Fisher information matrix corresponding to the target modal partitions. This leads to better estimates and improved correlation. Advantages of the method include its computationally nonintensive nature compared with exhaustive search techniques found in the literature and the benefit of physical insight into the ranking and ultimate selection of sensor locations. The method is successfully applied to the selection of sensor locations for identification and correlation of a set of target modes for the structural characterization of a proposed large space structure. The final sensor configuration provides superior Fisher information matrix trace, determinant, and condition number values compared to other methods of sensor selection.

Introduction

A KEY problem associated with the operation of proposed large space structures (LSSs) is the placement of sensors.[1] Because of weight and cost considerations, a minimum number must be placed in an optimum fashion. The sensors must be located such that the configuration fulfills the requirements of system identification, state estimation, and optimal control. Because of size and flexibility, LSSs can only be assembled on-orbit; therefore, extensive prelaunch analysis must be performed to verify the adequacy of the selected sensor configuration. Sensors cannot be easily moved after the LSS is in orbit.

A vast amount of literature has been produced dealing with the placement of sensors within a system. Methods have been developed to place sensors in an optimal fashion to address the problems of identification and control. Most of the contribution in this area deals with distributed parameter systems. Le Pourhiet and Le Letty[2] place sensors for system identification by maximizing the error sensitivity at each iteration with respect to the placement of a new sensor. Qureshi et al.[3] maximize the determinant of the Fisher information matrix associated with the parameters to be identified. Yu and Seinfield,[4] Omatu et al.,[5] and Sawaragi et al.[6] place sensors for state estimation by minimizing the trace of the estimate error covariance matrix. Sensor placement for optimal control is addressed by Goodson and Polis[7] by maximizing a measure of observability. A thorough review of the sensor placement literature concerning distributed parameter systems can be found in Kubrusly and Malebranche.[8]

Optimal sensor placement for the identification and control of large dynamic structures has been studied by Juang and Rodriguez,[9] Salama et al.,[10] and Baruh and Choe.[11] Number and sensor placement considering possible failures was investigated by Vander Velde and Carignan,[12] while sensor placement for the detection of dynamic changes in multivariable systems was studied by Basseville et al.[13,14] A relatively small number of papers have been written concerning the optimal placement of sensors for structural parametric identification such as those by Shah and Udwadia[15] and Udwadia and Garba.[16]

Received Sept. 12, 1989; revision received March 5, 1990.

*Assistant Professor, Department of Engineering Mechanics. Member AIAA.

This paper addresses the sensor placement problem from the standpoint of a structural dynamicist who must use the data collected from the sensors to validate an LSS finite element model (FEM). None of the papers found in the literature addresses this important problem. The sensors must be placed such that the data collected during an on-orbit vibration test will provide independent test-mode shapes and frequencies that can be compared with FEM modal parameters using test-analysis correlation techniques.[17] The FEM is then updated such that it accurately describes the real structure. It can then be used in structural dynamic analysis and control system synthesis.

Unlike most of the methods found in the literature, the method presented in this paper does not rely on computationally intensive exhaustive search techniques. Based on the prelaunch FEM, a set of target modes is selected for identification. The target mode set is assumed to include all modes that are strongly excited by the actuator configuration. An initial candidate set of sensor locations is also selected. The locations are then ranked based on their contribution to the linear independence of the corresponding FEM target mode partitions. Locations that do not contribute are removed from the candidate set. In an iterative manner, the initial candidate set of sensor locations is quickly reduced to the number of available sensors. The method therefore addresses the problem of selecting a given number of sensor locations from an initial much larger set such that the target mode partitions remain independent. Because of the iterative nature of the method, the final set of sensor locations is suboptimal. However, it is believed that the results based on the final configuration are close to the results that would be obtained from the actual optimal set.

The remainder of this paper describes the method and associated theory. A numerical example of the application of the method to the placement of sensors on an LSS is also presented.

Theoretical Formulation

This section presents a methodology for selecting an optimum set of sensor locations for identification and correlation of a given set of target modes. Initially, a candidate set of sensor locations is selected. This candidate set should be large enough to include all of the important dynamics within the target modes that are to be identified by the experiment. Perhaps it will include as many as 500 candidate locations.

However, it is assumed that the placement of 500 sensors on the structure is impossible; therefore, the initial candidate set must be reduced to an allotted number of sensor locations in an optimal fashion.

In this application, the candidate set is selected based on the modal kinetic energy distribution that gives a measure of the dynamic contribution of each FEM physical degree of freedom to each of the target mode shapes. This distribution is computed using the relation

$$\mathrm{KE}_{in} = \Phi_{in} \sum_j M_{ij}\, \Phi_{jn} \tag{1}$$

where KE_{in} is the kinetic energy associated with the ith degree of freedom in the nth target mode, Φ_{in} is the ith coefficient in the corresponding mode, M_{ij} is the term in the ith row and jth column of the FEM mass matrix, and Φ_{jn} is the jth coefficient in the nth mode. If the values of KE_{in} are added over all degrees of freedom and if the target modes are normalized to unit mass, the total will equal 1.0 corresponding to the generalized mass. The candidate set of sensor locations should result in a total kinetic energy of sufficient value for each of the target modes. No work has yet been performed to determine just how much kinetic energy for each target mode is required within the candidate set. Perhaps as little as 40–50% would be sufficient.

For the purpose of test-analysis correlation, the analyst must obtain measurements at locations on the structure that render the extracted test-mode partitions linearly independent. The test modes must be spatially differentiable. If the test-mode shapes are not spatially independent, test-analysis mode shape correlation using orthogonality and cross-orthogonality computations[18] cannot be performed because the test modes and the corresponding FEM modal partitions will be indistinguishable. Spatial independence implies that at any instant of time, if the sensor output equation is given by

$$u_s = \Phi_s q \tag{2}$$

the sensors can be sampled and an estimate can be computed for the target states $\hat{q}$ by solving Eq. (2) yielding

$$\hat{q} = [\Phi_s^T \Phi_s]^{-1} \Phi_s^T u_s \tag{3}$$

where u_s is the output from the sensors, Φ_s the matrix of FEM target modes partitioned to the sensor locations, and q the vector of target modal coordinates. Therefore, the states corresponding to the target modes must not only be observable from a control dynamics viewpoint,[19] they must also be absolutely identifiable.[2] It is assumed that the initial candidate set of sensor locations renders the modal partitions Φ_s linearly independent.

If the candidate sensor set contains s locations, but available resources limit the sensor configuration to $m < s$ sensors, the problem addressed in this paper is how to place the m sensors within the s candidate locations while maintaining as much independent information as possible and, thus, obtaining the best estimates of the modal states. The best estimate implies that the covariance matrix of the estimate errors will be a minimum. Following the development of Udwadia and Garba,[16] a modification of the output Eq. (2) is introduced as

$$u_s = H(q) + N = \Phi_s q + N \tag{4}$$

where the symbol H represents the process measurement and vector N represents stationary Gaussian white noise variance Ψ_o^2. For an efficient unbiased estimator, the covariance matrix of the estimate error is given by

$$P = E[(q - \hat{q})\,(q - \hat{q})^T] = \left[\left(\frac{\partial H}{\partial q}\right)^T [\Psi_o^2]^{-1} \left(\frac{\partial H}{\partial q}\right)\right]^{-1} \tag{5}$$

in which E denotes the expected value.

In this formulation it will be assumed that the sensors measure displacement, but similar results are obtained for velocity and acceleration measurement. Therefore, given $H(q) = \Phi_s\, q$, the covariance matrix is given by

$$P = [\Phi_s^T\, (\Psi_o^2)^{-1}\, \Phi_s]^{-1} = Q^{-1} \tag{6}$$

in which Q is the Fisher information matrix.[20] Maximizing Q would lead to the minimization of the covariance matrix and, thus, the best state estimate $\hat{q}$. To simplify the analysis, it is assumed that the measurement noise is uncorrelated and possesses identical statistical properties of each sensor. The Fisher information matrix can then be expressed as

$$Q = \frac{1}{\Psi_o^2}\, \Phi_s^T\, \Phi_s = \frac{1}{\Psi_o}\, A_o \tag{7}$$

Therefore, to minimize P, a suitable norm of A_o must be maximized. References 4 and 16 suggested the trace norm as the most useful and physically meaningful matrix norm. According to corollary 3 of Ref. 21, the determinant of the Fisher information matrix for the best linear estimate is largest for all linear unbiased estimators. In the sequel, A_o will be referred to as the Fisher information matrix.

In terms of the contribution of each degree of freedom, A_o can be expressed as

$$A_o = \sum_{i=1}^{s} \Phi_s^{iT}\, \Phi_s^i = \sum_{i=1}^{s} A^i \tag{8}$$

where Φ_s^ii is the ith row of the modal partition Φ_s corresponding to the ith degree of freedom or sensor location. Equation (8) illustrates that as each degree of freedom is added or subtracted from the candidated set, information is added to or subtracted from the Fisher information matrix. The number of degrees of freedom in the candidate sensor set can be reduced by eliminating locations that do not contribute significantly to the independent information contained within the target-mode partitions. Redundant information can be deleted.

The analysis begins by solving the eigenvalue equation

$$[A_o - \lambda\, I]\Psi = 0 \tag{9}$$

The k columns in Φ_s corresponding to the target modes are assumed to be linearly independent for the initial candidate sensor set. Therefore, the $k \times k$ matrix A_o is positive definite as well as symmetric. The eigenvalues of A_o are then real and positive, and the eigenvectors Ψ are orthonormal resulting in the relations

$$\Psi^T A_o \Psi = \lambda \qquad \text{and} \qquad \Psi^T \Psi = I \tag{10}$$

Because the vectors Ψ are orthogonal, they represent k orthogonal directions in a k-dimensional space, which will be called the absolute identification space. Forming the product

$$G = [\Phi_s\, \Psi] \otimes [\Phi_s\, \Psi] \tag{11}$$

where the symbol $\otimes$ represents a term-by-term matrix multiplication, results in matrix G in which each row contains the square of the components of the rows of Φ_s in terms of the coordinate system defined by the columns of Ψ, which span the absolute identification space. Each column of G sums to the corresponding eigenvalue of A_o. Thus, the ith term within a column represents the contribution of the ith sensor location to the associated eigenvalue. If G is postmultiplied by the inverse of the matrix of eigenvalues λ such that

$$F_E = [\Phi_s\, \Psi] \otimes [\Phi_s\, \Psi]\lambda^{-1} \tag{12}$$

each direction within the absolute identification space is now of equal importance. The ith term in the jth column of the

$s \times k$ matrix F_E represents the fractional contribution of the ith sensor location of the jth eigenvalue. Matrix F_E will be referred to as the fractional eigenvalue distribution. Addition of the terms within each row of F_E results in

$$E_D = \left[\sum_{j=1}^{k} F_{E1j} : \sum_{j=1}^{k} F_{E2j} : \cdots : \sum_{j=1}^{k} F_{Esj} \right]^T \tag{13}$$

in which F_{Eij} represents the jth term in the ith row of matrix F_E. Column vector E_D will be referred to as the effective independence distribution of the candidate sensor set. It is hypothesized that the ith term within E_D is the fractional contribution of the ith sensor location to the linear independence of the modal partitions Φ_s.

A better feel for the physical significance of the vector E_D can be obtained by considering a k-dimensional ellipsoidal surface defined by

$$x^T \lambda^{-1} x = 1 \tag{14}$$

which is referred to in the sequel as the absolute identification ellipsoid. The principal directions of this ellipsoid are given by the eigenvectors Ψ, and the length of the ith principal axis is $\lambda_i^{1/2}$. The magnitude of the ith eigenvalue gives a measure of how identifiable or how independent the modal partitions are if they are observed along the corresponding principal axis. If one of the eigenvalues becomes zero as sensor locations are deleted from the candidate set, the ellipsoid collapses, its volume vanishes, and the modal partitions Φ_s are no longer linearly independent. The volume of the identification ellipsoid is proportional to the square root of the determinant of A_o.[22] Following the formulation of Ref. 23, the determinant of A_o can be considered as formally analogous to the definition of information.[24] Therefore, as sensor locations are removed from the candidate set, it is desirable to maintain the determinant of A_o and, thus, the volume of the absolute identification ellipsoid.

The independence distribution vector E_D can be alternatively formulated as the diagonal of the matrix

$$E = \Phi_s \Psi \lambda^{-1} \Psi^T \Phi_s^T = \Phi_s A_o^{-1} \Phi_s^T \tag{15}$$

Using Eq. (10), E can be written as

$$E = \Phi_s [\Phi_s^T \Phi_s]^{-1} \Phi_s^T \tag{16}$$

The matrix E in Eq. (16) can be identified as an orthogonal projector[25] onto the column space of Φ_s with rank equal to the number of target modes. The projector E is also an idempotent matrix,[25] which means that $E^2 = E$. A well-known characteristic of idempotent matrices is that their trace is equal to their rank. Therefore, the terms on the diagonal of E and also within E_D represent the contributions of the corresponding sensor locations to the rank of Φ_s or the linear independence of its columns as hypothesized.

If the diagonal terms within matrix E are further examined, the ith term is of the form

$$E_{ii} = \rho_i^T \lambda^{-1} \rho_i \tag{17}$$

in which ρ_i is a column vector containing the ith row of Φ_s expressed in terms of the coordinates Ψ. Equation (17) represents the square of the ellipsoidal norm of the ith row of Φ_s with respect to coordinates Ψ using metric λ^{-1}. Each row of the modal partition Φ_s can be plotted as a vector in the identification space and it is hypothesized that each of these vectors will lie within the absolute identification ellipsoid such that

$$0.0 \le E_{ii} \le 1.0$$

If $E_{ii} = 0.0$, the ith row of Φ_s is null and obviously the modes are not observable from the corresponding sensor location. If the ellipsoidal length of the ith row of Φ_s is 1.0, the corresponding vector's tip will touch the surface of the identification ellipsoid and it is also hypothesized that the corresponding sensor location is vital to the linear independence and, thus, the identification of the target modes.

As a simple example, consider two modes measured at three sensor locations given by

$$\Phi_s = \begin{bmatrix} 1 & 2 \\ 1 & 1 \\ 1 & 1 \end{bmatrix}$$

The eigenvalues of A_o are given by $\lambda_1 = 0.228$ and $\lambda_2 = 8.772$ with corresponding eigenvectors

$$\Psi_1 = \begin{bmatrix} 0.8219 \\ -0.5696 \end{bmatrix} \qquad \Psi_2 = \begin{bmatrix} 0.5696 \\ 0.8219 \end{bmatrix}$$

The rows of Φ_s are plotted in the absolute identification space along with the corresponding identification ellipsoid in Fig. 1. Note that row 1, ρ_1, touches the surface of the ellipsoid while rows 2 and 3, ρ_2 and ρ_3, are interior to the surface. The corresponding effective independence vector is given by

$$E_D = \begin{bmatrix} 1.0 \\ 0.5 \\ 0.5 \end{bmatrix}$$

indicating that sensor location 1 is vital to the linear independence and identification of the mode shapes, whereas sensor locations 2 and 3 are of equal importance and either one could be eliminated without affecting the independence of the modes. These results are obvious from inspection of the coefficients in Φ_s. The modal coefficients corresponding to the first sensor location spatially distinguished the modes. Eliminating it would render the modal partitions dependent. The remaining two rows possess like coefficients; therefore, their effective independence is the same, and inclusion of both would retain redundant information. This simple example thus supports the hypotheses. It is clear from the example that the effective independence distribution can be used to rank the importance of sensor locations within the initial candidate set.

The necessity of retaining any row that touches the identification ellipsoid will now be proven for the general case. Suppose that R_i is a column vector containing the ith row of the modal partition Φ_s. Assume that the ith row touches the identification ellipsoid such that

$$E_{ii} = R_i^T \Psi \lambda^{-1} \Psi^T R_i = R_i^T A_o^{-1} R_i$$
$$= < R_i, A_o^{-1} R_i > = 1.0 \tag{18}$$

in which $<,>$ denotes the usual inner product for column vectors. If all of the candidate sensor locations are retained, A_o is nonsingular. The ith sensor location is vital to the linear independence of the modal partitions if the elimination of the

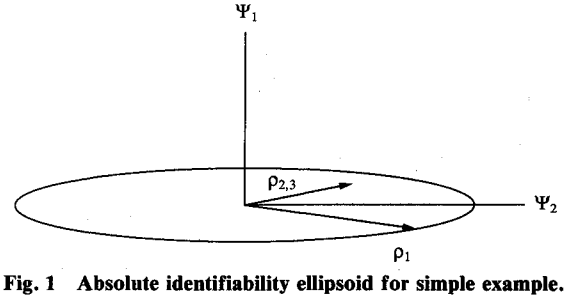

Fig. 1 Absolute identifiability ellipsoid for simple example.

term A^i in the series of Eq. (8) results in a singular matrix. The analysis proceeds by forming the matrix B such that

$$B = A_o - A^i = A_o - R_i R_i^T \tag{19}$$

Premultiplying by the inverse of A_o results in the matrix C

$$C = A_o^{-1}[A_o - A^i] = I - A_o^{-1} R_i R_i^T \tag{20}$$

where I denotes an identity matrix of order k. Note that the rank of C is identical to the rank of B. Taking the trace (tr) of both sides of Eq. (20) yields

$$\text{tr}(C) = \text{tr}(I) - \text{tr}(A_o^{-1} R_i R_i^T) \tag{21}$$

From Skelton[26] it is known that

$$<R_i, A_o^{-1} R_i> = \text{tr}>A_o^{-1}R_i, R_i < = \text{tr}(A_o^{-1} R_i R_i^T) \tag{22}$$

where $>,<$ denotes the outer product. Therefore, using Eqs. (18), (21), and (22) it can be seen that $\text{tr}(C) = k - 1$. Next, transpose C and introduce the matrix P_i such that

$$C^T = I - R_i R_i^T A_o^{-1} = I - P_i \tag{23}$$

Examining P_i, the following relation can be derived:

$$P_i^2 = P_i P_i = R_i R_i^T A_o^{-1} R_i R_i^T A_o^{-1} = R_i < R_i$$

$$A_o^{-1} R_i > R_i^T A_o^{-1} = R_i R_i^T A_o^{-1} P_i \tag{24}$$

Equation (24) indicates that the matrix P_i is also idempotent, therefore, the trace of P_i is equal to its rank (rk). Due to a one-to-one correspondence between idempotent matrices and projectors,[25] P_i is also seen to be an oblique projector onto a range space spanned by R_i along the corresponding null space of P_i as illustrated by the equation

$$P_i R_i = R_i R_i^T A_o^{-1} R_i = R_i <R_i, A_o^{-1} R_i> = R_i \tag{25}$$

Therefore, $C^T = I - P_i$ is the corresponding oblique projector onto the null space along the range space and, thus, is also idempotent. The final result yields

$$\text{tr}(C^T) = \text{rk}(C^T) = \text{rk}(C) = \text{rk}(B) = k - 1 \tag{26}$$

the matrix B is $k \times k$ and of rank $k - 1$; therefore B is singular and the sensor location corresponding to R_i and thus A^i must be retained as hypothesized.

There is one more question which must be answered. Can a vector R_i extend beyond the identification ellipsoid? This would imply

$$<R_i, A_o^{-1} R_i> = R_i^T A_o^{-1} R_i = \sigma_i > 1.0 \tag{27}$$

the matrix B is formed as before and note that because B can be written as $B = \Phi_{si}^T \Phi_{si}$, it is at least positive semidefinite,[26] where Φ_{si} denotes the modal partitions Φ_s with the ith row removed. Thus, all the eigenvalues λ_{Bi} of B are greater than or equal to 0.0. Again form matrices C, C^T, and P_i and note that the sign-definiteness of B, C, and C^T are identical because A_o^{-1} is positive definite. The matrix product $P_i R_i$ is now of the form

$$P_i R_i = R_i R_i^T A_o^{-1} R_i = R_i <R_i, A_o^{-1} R_i> = R_i \sigma_i \tag{28}$$

which implies that σ_i is an eigenvalue of matrix P_i. The corresponding eigenvalue of C^T is given by

$$\lambda_{C^T i} = 1.0 - \sigma_i < 0.0$$

Therefore, matrices C^T and C have a negative eigenvalue and are thus not positive semidefinite. However, this implies that B is not positive semidefinite, which contradicts the original statement that matrix B must at least be positive semidefinite. This proves that vector R_i cannot extend through the identification ellipsoid.

Thus, a measure has been developed, called effective independence, which yields the contribution of a sensor location to the rank of the modal partitions Φ_s and, thus, the linear independence of its columns. The vector E_D of Eq. (13) can thus be used to rank sensor locations based on their importance to the identification and correlation of the target modes. A sensor location will have a contribution in the range

$$0.0 \leq E_{Di} \leq 1.0$$

If $E_{Di} = 0.0$, the sensor location does not contribute and the system is not even observable from the corresponding location. If $E_{Di} = 1.0$, the sensor location must be retained in the final sensor configuration in order to identify the target modes. In an iterative manner, the sensor locations in the current candidate set can be ranked, locations that do not contribute substantially can be identified, and then these locations can be eliminated from the target modal partitions Φ_s. Using this approach, sensor locations can be eliminated in a suboptimal manner to arrive at a final sensor configuration containing the allotted number of sensors that will give the best chance of accurately identifying and correlating the target modes.

The derived sensor configuration is said to be suboptimal because it is generated in an iterative manner, but it is believed that the suboptimal configuration will yield results that are close to those produced by the actual optimal sensor locations. The accuracy of the estimation or goodness of the sensor configuration can be monitored during the iteration process by tracking the trace of A_o, as suggested in Refs. 4 and 16, the determinant of A_o, which is a measure of the amount of information contained in the measurements, and the condition number[27] of A_o, which yields a measure of the estimation's robustness to modeling errors in the measurement matrix Φ_s derived from the FEM representation.

It is important to note that the effective independence value for each retained sensor changes after each iteration such that the sum of the terms in the column vector E_D remains equal to the number of target modes k. Individual locations become more or less important as ineffective sensor locations are iteratively removed. Order of importance may even be changed as certain sensors are deleted. The best approximation to the optimal sensor configuration can be achieved by deleting only one location per iteration. This approach minimizes the change in the effective independence value experienced by each retained sensor location from one iteration to the next. However, it is believed that more than one sensor can be deleted during an iteration in most cases. Deletion of large numbers of sensor locations during an iteration should be avoided. The number of sensor locations that can be removed safely during each iteration is a subject of further research.

Numerical Example

The method for ranking sensor locations presented in this paper was applied to locate sensors for structural characterization of the phase I configuration of the Space Station. The FEM representation is illustrated in Fig. 2. For demonstration purposes, 15 fundamental main truss bending modes were selected for identification and ultimate test-analysis correlation. Table 1 lists frequencies and descriptions for the 15 target modes. Selection of the initial candidate sensor set was based on modal kinetic energy. The kinetic energy for each FEM physical degree of freedom was computed for the 15 truss target-mode shapes. Degrees of freedom were then ranked according to their overall contribution to the target modes using a FORTRAN program.

The top 200 degrees of freedom were selected as the initial candidate set of sensor locations. The number 200 was selected

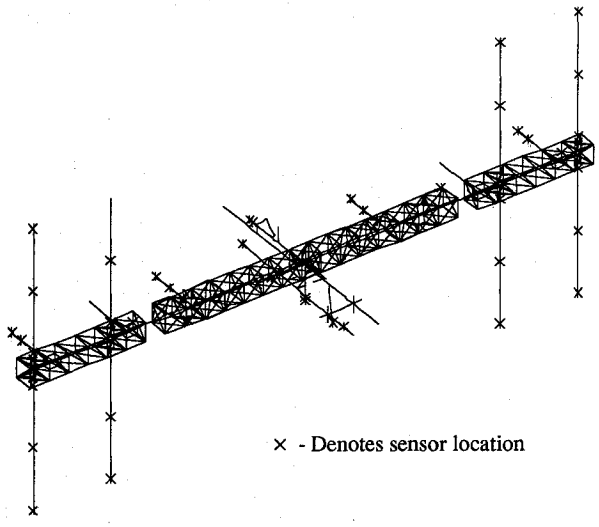

Fig. 2 Phase I configuration space station finite element model and selected sensor locations.

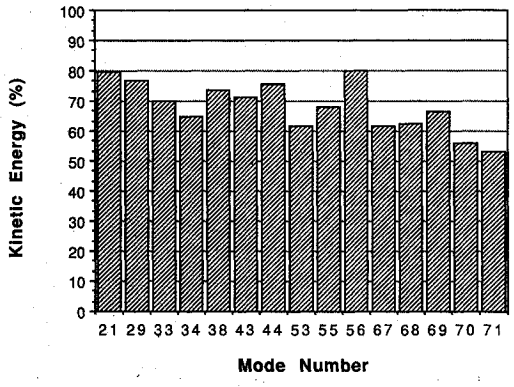

Fig. 3 Percentage of kinetic energy contained within candidate sensor location set (187 DOF) for each truss target mode.

arbitrarily and the ranking did not guarantee that the kinetic energy contained in these 200 degrees of freedom was evenly distributed over all the target modes. Because several of the degrees of freedom in the candidate set were located on common rigid bodies within the FEM, the set was immediately reduced to 187 independent candidate locations. Figure 3 presents the percentage of the total kinetic energy that is contained in the candidate set for all 15 target modes. Each mode possesses greater than 50% of its kinetic energy within the candidate set. Therefore, it is assumed that the candidate set is large enough to describe the target modes. To demonstrate the method, 70 sensor locations that would give the best estimates of the 15 truss target modes were to be selected from the candidate set of 187.

The number 70 was selected arbitrarily for the demonstration. However, this is a physically realistic number based on the common practice of having many more sensors than target modes for modal identification. The method presented in this paper indicates that mathematically only 15 sensors are required to identify the 15 target modes. In general, this is not possible due to the presence of model uncertainty, sensor noise, and possible sensor failures. The number of sensors required to guarantee identification of the target modes in the presence of errors, noise, and failures is a subject of further investigation.

Initial analysis ranked the importance of each sensor location within the candidate set of 187. The fractional eigenvalue distribution given by Eq. (12) is illustrated in a three-dimensional plot in Fig. 4. The abscissa of the plot represents the eigenvalues of the matrix A_o whereas the ordinate represents

Table 1 Frequencies and descriptions of 15 selected target truss modes

Mode	Frequency	Description of truss
21	0.124	First-order bending about x
29	0.144	First-order bending about z
33	0.158	First-order bending about z
34	0.160	First-order bending about x
38	0.331	Second-order bending about x
43	0.488	Second-order bending about z
44	0.513	Second-order bending about x
53	0.653	Third-order bending about z
55	0.722	Third-order beding about x
56	0.792	Port side torsion
67	1.169	Third-order bending (z)/torsion
68	1.242	Fourth-order bending (x)/torsion
69	1.257	Port side bending (x)/torsion
70	1.334	Torsion
71	1.352	Starboard side bending (z)/torsion

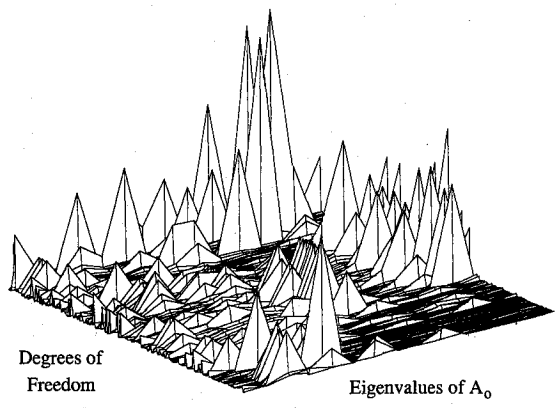

Fig. 4 Fractional eigenvalue distribution for initial 187-DOF candidate sensor set and 15 truss target modes.

the degrees of freedom in the candidate sensor location set. Each peak in the figure indicates the fractional contribution of each sensor location to the corresponding eigenvalue of A_o. Note that there are many sensor locations that do not contribute significantly to many of the eigenvalues. Adding the rows of F_E results in the effective independence of each sensor location, vector E_D given in Eq. (13). Figure 5 illustrates the effective independence for the initial candidate sensor set after entries within E_D have been sorted from highest to lowest value. The largest value is 0.493; therefore, no single sensor location is absolutedly vital to the independence of the target modes. However, several sensor locations possess insignificant contributions to the identification of the modes and, thus, can be immediately eliminated from the sensor set during the first iteration.

Seven iterations were performed to reduce the number of sensor locations from 187 to 70. Figure 6 illustrates the sorted E_D vector for each of the iterations. The area under each curve represents the rank of the corresponding matrix A_o, which is a constant 15.0 during all of the iterations. As sensor locations are removed, the remaining locations become more important to the independence of the modal partitions. If the truncation process was continued until there were as many sensors as target modes, the effective independence value for each remaining sensor location would be 1.0, indicating that the removal of an additional sensor would render the target modal partitions dependent.

The trace, determinant, and condition number of matrix A_o were monitored during the iteration sequence to track the goodness of the selected sensor sets. These matrix measures were also computed during a corresponding sensor truncation analysis using the usual straightforward method of truncation

based on kinetic energy. Figure 7 compares the trace values for each of the truncation analyses over the seven iterations. The method of effective independence clearly maintains a larger trace value of A_o than the kinetic-energy-based truncation method. Therefore, using the effective independence method results in a sensor configuration possessing a smaller estimate error covariance matrix yielding better state estimates. In the case of the determinant of A_o, the difference between the results of the effective independence method and the kinetic energy method is even more dramatic as illustrated in Fig. 8. The sensor configurations derived using the independence measure clearly retain more information than the configurations based on kinetic energy. Results for the condition number of A_o are presented in Fig. 9. The condition numbers for the independence-based configurations and the kinetic-energy-based configurations are comparable down to 80 sensor locations with the kinetic energy yielding slightly better results. However, below 80 locations, the method of effective independence yields a configuration with a much smaller condition number than the corresponding kinetic energy configuration, which results in less sensitivity in the estimates to analytical modeling error. Also, the condition number resulting form the independence technique seems to be much more stable and predictable than the condition number resulting from sensor truncation based on kinetic energy.

The sensor locations retained in the final set of 70 are listed in Table 2 and illustrated in Fig. 2. Note that many of the important sensor locations are on the photovoltaic (PV) arrays. This is because the fundamental truss modes possess a substantial amount of PV array motion. Thus, they are highly visible from the PV arrays. Table 3 lists the effective indepen-

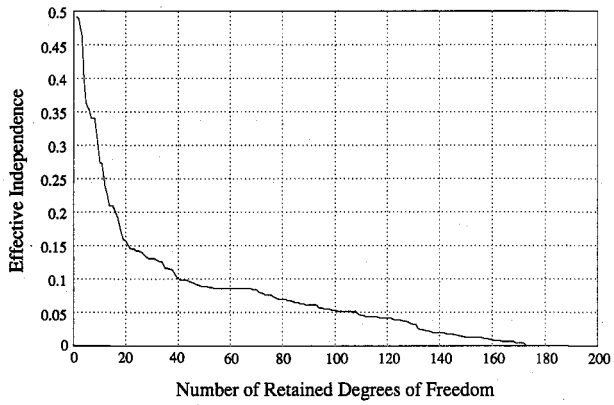

Fig. 5 Effective independence distribution for initial 187-DOF candidate sensor set and 15 truss target modes.

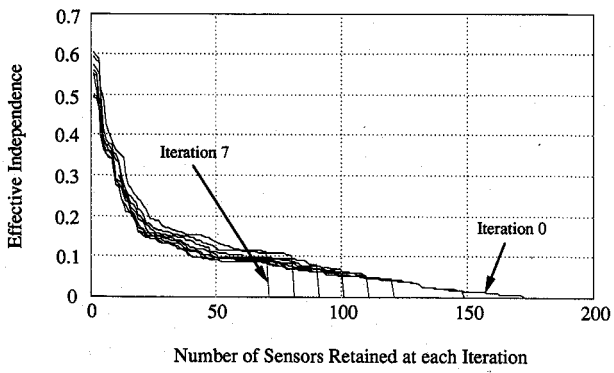

Fig. 6 Effective independence distribution for all seven iterations.

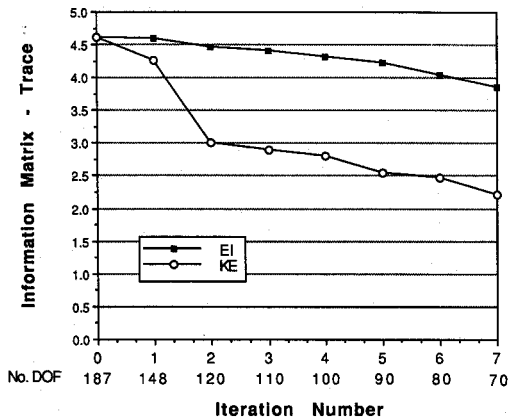

Fig. 7 Trace of matrix A_o vs iteration of sensor configurations.

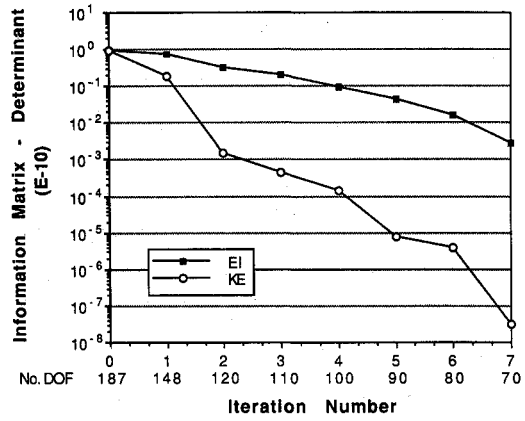

Fig. 8 Determinant of matrix A_o vs iteration of sensor configurations.

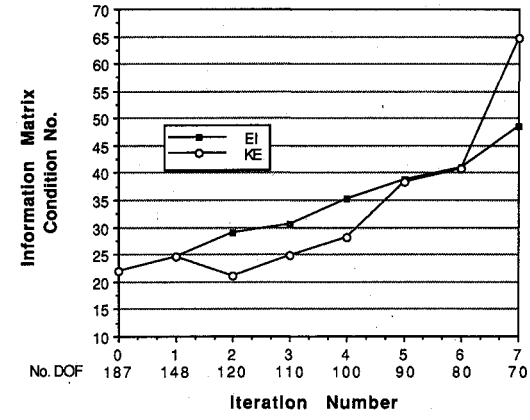

Fig. 9 Condition number of matrix A_o vs iteration of sensor configurations.

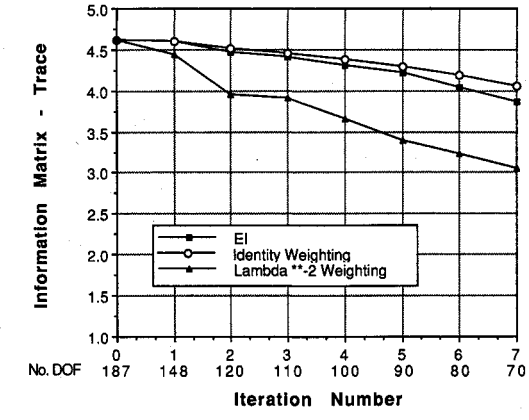

Fig. 10 Comparison of Fisher information matrix trace values vs iteration for identity weighting, effective independence, and λ^{-2} weighting.

Table 2 Seventy-degree-of-freedom (DOF) sensor configuration for identification of 15 target truss modes

Grid ID	DOF	Location
289	2	Port outboard EPS radiator
290	23	Port outboard EPS radiator
293	2	Stbd[a] outboard EPS radiator
294	2	Stbd outboard EPS radiator
317	3	Stbd station radiator
318	23	Stbd station radiator
319	23	Stbd station radiator
322	3	Port station radiator
323	23	Port station radiator
324	23	Port station radiator
378	1	Port antenna
382	1	Stbd lower RCS[b]
5017	3	Exposed facility
5018	23	Exposed facility
8002	1	Stbd outboard PV[c] array base
8003	1	Stbd outboard PV array
8006	1	Stbd outboard PV array
8009	23	Stbd outboard PV array tip
8015	1	Stbd outboard PV array
8016	1	Stbd outboard PV array
8019	12	Stbd outboard PV array
8022	12	Stbd outboard PV array tip
8032	1	Stbd inboard PV array
8035	2	Stbd inboard PV array tip
8042	1	Stbd inboard PV array
8045	1	Stbd inboard PV array
8054	1	Port outboard PV array base
8055	13	Port outboard PV array
8058	123	Port outboard PV array
8061	123	Port outboard PV array tip
8067	13	Port outboard PV array
8068	13	Port outboard PV array
8071	123	Port outboard PV array
8074	23	Port outboard PV array tip
8081	1	Port inboard PV array
8084	1	Port inboard PV array
8087	2	Port inboard PV array tip
8097	1	Port inboard PV array
8100	2	Port inboard PV array tip
8507	1	IEA
8521	13	IEA
8531	13	IEA
30104	2	HAB mounted SSRMS
39828	3	Aft nodes—module cluster
39831	2	Aft nodes—module cluster
39832	2	Aft nodes—module cluster
39835	3	Aft nodes—module cluster
39842	3	ESA module
39893	3	Docking structure

[a]Starboard [b]Reaction control system [c]Photovoltaic

dence value associated with each of these sensor locations. If this set of 70 is indeed the final sensor configuration, Table 3 lists the cost of losing each sensor. This information can be used to place backup sensors. For example, the loss of the sensor at grid number 294 in direction 2(y) would have the greatest impact on any on-orbit experiment.

It is also of interest to look at the effect of the weighting matrix λ^{-1} in Eq. (12) on the effective independence distribution and the matrix measures of A_o as the iterative truncation of sensor locations proceeds. Therefore, two more sensor truncation analyses were performed for the Space Station example. The first additional analysis substituted an identity matrix for the weighting matrix λ^{-1} in Eq. (12), while the second analysis used the weighting matrix λ^{-2}. The resulting trace, determinant, and condition number of the Fisher information matrix A_o at each iteration for the additional analyses were compared with the corresponding results previously derived for the straightforward effective independence method.

The trace values are compared in Fig. 10. Note that the use of an identity weighting matrix yields the largest trace values.

Table 3 Effective independence (EFI) distribution for 70-degree-of-freedom sensor configuration

Number	DOF	EFI
1.00	294.20	0.61
2.00	290.20	0.59
3.00	290.30	0.59
4.00	319.30	0.51
5.00	8009.30	0.49
6.00	324.30	0.43
7.00	8006.10	0.41
8.00	8071.10	0.39
9.00	319.20	0.38
10.00	39835.30	0.36
11.00	324.20	0.35
12.00	8019.20	0.35
13.00	8019.10	0.34
14.00	8058.10	0.30
15.00	289.20	0.27
16.00	318.30	0.27
17.00	293.20	0.25
18.00	323.30	0.24
19.00	8045.10	0.24
20.00	30104.20	0.24
21.00	8097.10	0.22
22.00	8032.10	0.22
23.00	8016.10	0.20
24.00	8084.10	0.19
25.00	5018.30	0.19
26.00	8003.10	0.19
27.00	39832.20	0.19
28.00	8015.10	0.18
29.00	8074.20	0.17
30.00	8061.20	0.17
31.00	8002.10	0.17
32.00	5018.20	0.17
33.00	8100.20	0.17
34.00	8521.30	0.16
35.00	8055.10	0.16
36.00	8071.20	0.16
37.00	8068.10	0.16
38.00	39831.20	0.15
39.00	8531.30	0.15
40.00	378.10	0.15
41.00	8058.20	0.15
42.00	8087.20	0.15
43.00	318.20	0.15
44.00	322.30	0.15
45.00	323.20	0.15
46.00	8054.10	0.15
47.00	5017.30	0.15
48.00	8067.10	0.14
49.00	8521.10	0.14
50.00	39893.30	0.14
51.00	8061.10	0.13
52.00	8081.10	0.13
53.00	8009.20	0.13
54.00	39842.30	0.13
55.00	317.30	0.13
56.00	8035.20	0.12
57.00	382.10	0.12
58.00	8022.10	0.12
59.00	8074.30	0.12
60.00	8061.30	0.12
61.00	8071.30	0.12
62.00	8058.30	0.12
63.00	8068.30	0.12
64.00	8067.30	0.12
65.00	8055.30	0.12
66.00	8042.10	0.12
67.00	8531.10	0.11
68.00	8507.10	0.11
69.00	8022.20	0.11
70.00	39828.30	0.11

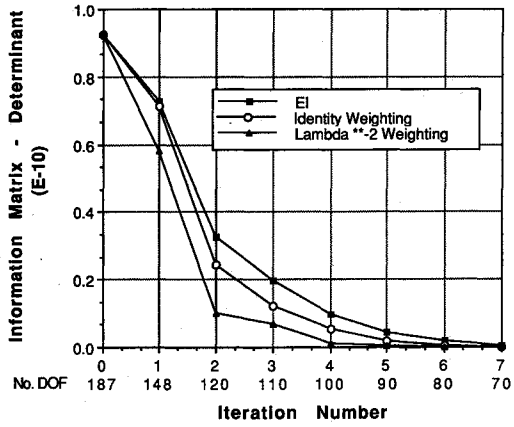

Fig. 11 Comparison of Fisher information matrix determinant values vs iteration for identity weighting, effective independence, and λ^{-2} weighting.

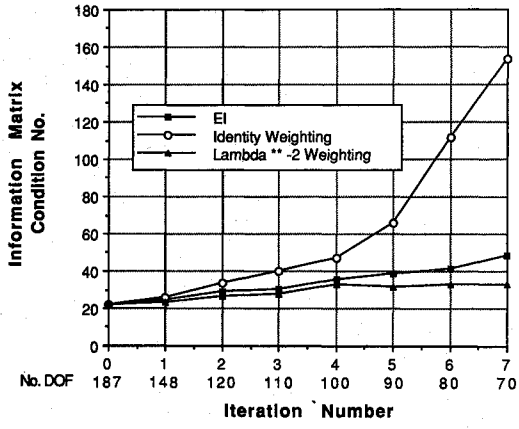

Fig. 12 Comparison of Fisher information matrix condition number values vs iteration for identity weighting, effective independence, and λ^{-2} weighting.

However, the values derived from effective independence come close to duplicating these results for the trace. Using λ^{-2} as a weighting matrix yields substantially smaller trace values. Determinant values for each weighting matrix option are plotted vs iteration number in Fig. 11. In this case the effective independence method gives the largest values of the Fisher information matrix determinant. Therefore, λ^{-1} provides the proper weighting for maximizing retained information, which will yield the best estimates. Finally, the condition number of the Fisher information matrix is compared for all three analyses in Fig. 12. In this case, the weighting matrix λ^{-2} outperforms the other two analyses yielding smaller values of the condition number for the Fisher information matrix. But again, it is interesting to note that the values derived from truncating the sensor locations based on the effective independence method closely approximate the results obtained using weighting matrix λ^{-2}. Therefore, while the method yields the largest values of the Fisher information matrix determinant, it also closely approximates the best results for the other two matrix measures, trace and condition number. Thus, the effective independence method seems to yield the best overall results.

Conclusion

A method for sensor placement was presented that is based on ranking the contribution of each candidate sensor location to the linear independence of the corresponding target modal partitions. In an iterative fashion, locations that do not contribute significantly to the independent information contained within the target modes are removed. Within a relatively small number of iterations, the initial candidate set of sensor locations can be reduced to the allotted number in a suboptimal manner. The method, called effective independence, results in a sensor truncation process that maximizes the determinant of the Fisher information matrix. This maximizes retained independent information and tends to minimize the covariance matrix of the estimate errors, thus giving the best state estimates of the target modes. The main advantage of the method of sensor placement presented in this paper is that it is computationally nonintensive compared with the exhaustive search techniques found in the literature. An eigenvalue solution of only a relatively small matrix with order corresponding to the number of target modes must be performed. All of the analysis using the method of effective independence presented in this paper was performed on a Macintosh II using MATLAB. It is also believed that the method offers the benefit of physical insight into the ranking and ultimate selection of sensor locations. It is important to note that in its present form the method of effective independence does not determine how many sensors are required to identify the target modes in the presence of model uncertainty, sensor noise, high modal density, and sensor failure. The number of sensors required to guarantee identification of the target modes is a subject of further research. The question may ultimately be answered by simulating the actual on-orbit experiment and extracting mode shapes and frequencies from the resulting simulated test data. However, the method can be used to place a set of sensors within a larger candidate set in a suboptimal manner.

Acknowledgment

This research was partially supported by Structural Dynamics Research Corporation, San Diego, CA.

References

[1]Denman, E., Hassleman, T., Sun, C. T., Juang, J.-N., Junkins, J., Udwadia, F., Venkayya, V., and Kamat, M., "Identification of Large Space Structures on Orbit," American Society of Mechanical Engineers, New York, AFRPL TR-86-054, Sept. 1986.

[2]Le Pourhiet, A., and Le Letty, L., "Optimization of Sensor Locations in Distributed Parameter System Identification," *Identification and System Parameter Estimation,* edited by Rajbman, North-Holland, Amsterdam, 1978, pp. 1581-1592.

[3]Qureshi, Z. H., Ng, T. S., and Goodwin, G. C., "Optimum Experimental Design for Identification of Distributed Parameter Systems," *International Journal of Control,* Vol. 31, No. 1, 1980, pp. 21-29.

[4]Yu, T. K., and Seinfeld, J. H., "Observability and Optimal Measurement Locations in Linear Distributed Parameter Systems," *International Journal of Control,* Vol. 18, No. 4, 1973, pp. 785-799.

[5]Omatu, S., Koide, S., and Soeda, T., "Optimal Sensor Location for Linear Distributed Parameter Systems," *IEEE Transactions on Automatic Control,* Vol. AC-23, No. 4, 1978, pp. 665-673.

[6]Sawaragi, Y., Soeda, T., and Omatu, S., *Modeling, Estimation and Their Application for Distributed Parameter Systems,* Lecture Notes in Control & Information Science, Vol. 11, 1978, Springer-Verlag, Berlin, Germany.

[7]Goodson, R. E., and Polis, M. P., "Identification of Parameters in Distributed Systems," *Distributed Parameter Systems,* edited by W. H. Ray and D. G. Lainiotis, Dekker, New York, 1978.

[8]Kubrusly, C. S., and Malebranche, H., "Sensors and Controllers Location in Distributed System—A Survey," *Automatica*, Vol. 21, No. 2, 1985, pp. 117-128.

[9]Juang, J.-N., and Rodriguez, G., "Formulations and Applications of Large Structure Actuator and Sensor Placements," *Proceedings of the 2nd VPI&SU/AIAA Symposium on Dynamics and Control of Large Flexible Spacecraft,* Virginia Polytechnic Inst. and State Univ., Blacksburg, VA, June 1979, pp. 247-262.

[10]Salama, M., Rose, T., and Garba, J., "Optimal Placement of Excitation and Sensors for Verification of Large Dynamical Systems," *Proceedings of the AIAA/ASME/ASCE/AHS 28th Structures, Structural Dynamics, and Materials Conference,* AIAA, New York, 1987, pp. 1024-1031.

[11]Baruh, H., and Choe, K., "Sensor Placement in Strucutral Control," AIAA Paper 88-4056, 1988.

[12]Vander Velde, W. E., and Carignan, C. R., "Number and Place-

ment of Control System Components Considering Possible Failures," *Journal of Guidance, Control, and Dynamics,* Vol. 7, No. 6, 1984, pp. 703–709.

[13]Basseville, M., Benveniste, A., Moustakides, G., and Rougee, A., "Detection and Diagnosis of Changes in the Eigenstructure of Nonstationary Multivariable Systems," *Automatica,* Vol. 23, July 1987, pp. 479–489.

[14]Basseville, M., Benveniste, A., Moustakides, G., and Rougee, A., "Optimal Sensor Location for Detecting Changes in Dynamical Behavior," *IEEE Transactions on Automatic Control,* Vol. AC-32, No. 12, 1987, pp. 1067–1075.

[15]Shah, P. C., and Udwadia, F. E., "A Methodology for Optimal Sensor Locations for Identification of Dynamic Systems," *Journal of Applied Mechanics,* Vol. 45, March 1978, pp. 188–196.

[16]Udwadia, F. E., and Garba, J. A., "Optimal Sensor Locations for Structural Identification," *JPL Proceedings of the Workshop on Identification and Control of Flexible Space Structures,* April 1985, pp. 247–261.

[17]Kammer, D. C., Jensen, B. M., and Mason, D. R., "Test-Analysis Correlation of the Space Shuttle Solid Rocket Motor Center Segment," *Journal of Spacecraft and Rockets,* Vol. 26, No. 4, 1989, pp. 266–273.

[18]Chen, J. C., and Garba, J. A., "Structural Analysis Model Validation Using Modal Test Data," *Proceedings of the Joint ASCE/ASME Conference,* June 1985, pp. 109–137.

[19]Hughes, P. C., and Skelton, R. E., "Controllability and Observability of Linear Matrix-Second-Order Systems," *Journal of Applied Mechanics,* Vol. 47, June 1980, pp. 415–420.

[20]Middleton, D., *An Introduction to Statistical Communication Theory,* McGraw-Hill, New York, 1960.

[21]Fedorov, V. V., *Theory of Optimal Experiments,* translated and edited by W. J. Studden and E. M. Klimko, Academic, New York, 1972, p. 28.

[22]Battin, R. H., *An Introduction to the Mathematics and Methods of Astrodynamics,* AIAA, New York, 1987, p. 668.

[23]Johnson, C. D., "Optimization of a Certain Quality of Complete Controllability and Observability for Linear Dynamical Systems," *Transcripts of the American Society of Mechanical Engineers,* Series-D, Vol. 91, June 1969, pp. 228–237.

[24]Shannon, C. E., "Mathematical Theory of Communication," *Bell System Technical Journal,* Vol. 27, No. 3, 1948, pp. 379, 623.

[25]Ben-Israel, A., and Greville, T. N. E., *Generalized Inverses: Theory and Application,* Wiley, New York, 1974, p. 11.

[26]Skelton, R. E., *Dynamics Systems Control, Linear Systems Analysis and Synthesis,* Wiley, New York, 1988, p. 52.

[27]Ortega, J. M., and Poole, W. G., Jr., *An Introduction to Numerical Methods for Differential Equations,* Pitman, Marshfield, MA, 1981.